DEVELOPMENT OF A PREDICTIVE MODEL FOR THERMAL CONDUCTIVITY IN GRAPHENE NANOPLATELETS-INFUSED DAMPER OIL USING ANN/RSM

Manikandan S[1], Nanthakumar A.J.D [*1]

[1]Vehicle Dynamics Laboratory, Department of Automobile Engineering, College of Engineering and Technology, SRM Institute of Science and Technology, Kattankulathur Campus, Chengalpattu-603203, Tamilnadu, India.

[*] Corresponding author; E-mail: ajd.nanthakumar@gmail.com

This study aims to develop a predictive model for the thermal conductivity of graphene nanoplatelets/SAE10W oil nanofluids using artificial neural networks and response surface methodology. Generally, the property of thermal conductivity has been measured to enhance the heat transfer efficiency of traditional heat transfer fluids. Experiments were conducted using a thermal constants analyzer at different operating conditions, such as varying the volume concentrations of nanoparticles from 0.050% to 0.150% and increasing the temperature from 20°C to 80°C. Results showed an improvement in the thermal conductivity of the nanofluid, ranging from 19% to 41%. A single hidden layer with 12 neurons was found to be the most effective architecture for the artificial neural network model. Additionally, a response surface was closely fitted to experimental data points in the response surface methodology. Then, mean squared error, root mean square error, and R-squared values were employed to validate the accuracy of the predicted models. The correlation coefficients of the artificial neural network and response surface methodology models were 0.99761 and 0.9877, respectively. Also, the accuracy of the models was assessed in terms of margins of deviation. The margin of deviation for the artificial neural network model ranged between +0.3926% and -0.4640%, whereas for the response surface methodology model, it was between +0.4137% and -0.4166%. The comparison of the artificial neural network model indicates greater accuracy than the response surface methodology technique. This method for predicting the thermal conductivity of graphene nanoplatelets /SAE10W oil nanofluids is both cost-effective and inventive, minimizing experimental research durations.

Key words*: Thermal conductivity, Artificial neural network, Response surface methodology, Graphene nanoplatelets.*

1. Introduction

Nanofluids play a pivotal role in technological advancements across scientific domains with their applications continually expanding. Enhancing the heat transfer efficiency of common fluids such as water, ethylene glycol (EG), and other fluids is difficult due to their inherent low thermal conductivity [1–3]. Consequently, a prominent area within nanotechnology focuses on augmenting the characteristics of heat transfer fluids[4–6]. The processes of heat transfer play a vital role in numerous industrial applications such as electronic components, automotive, industrial and energy sectors. Nanofluids are comprised of colloidal suspensions of nanoparticles within a base fluid, resulting in improved properties of the base fluid and an elevated heat transfer rate [7–10]. Nanofluid particles comprise diverse metals, metal oxides, and carbon nanotubes under development to attain more effective heat transfer compared to conventional fluids. In their study, Choi *et al*. [11] found that the dispersion of copper (Cu) nanoparticles in water resulted in an improvement in the thermal conductivity of Cu/water nanofluids. Thermal conductivity was recognized as the most pivotal property for enhancing heat transfer rates. Several experiments were conducted to investigate the influence of various parameters, including size, shape, volume concentration (Φ), temperature (T) and surfactants, on the thermophysical properties of nanofluids.

Over the past few decades, many researchers have investigated nanofluid thermal conductivity using mathematical models based on both experimental and theoretical data. Despite this, applying Maxwell's model, which is primarily intended for microparticle-based fluids, to other nanofluids results in significant deviations from experimentally measured thermal conductivity. Subsequently, several thermophysical models such as Hamilton-Crosser, Bruggeman, Yu and Choi, and Pak and Cho have been employed to improve prediction accuracy [12, 13]. Nevertheless, significant discrepancies persist in predicting nanofluid thermophysical properties as these models rely on conventional tools and cannot accurately forecast nanofluid properties under varying conditions using correlations developed solely from experimental data.

Computer science and software advancements have resulted in the development of different approaches for predicting the characteristics of nanofluids in recent years. These approaches include artificial neural network (ANN), genetic, fuzzy logic algorithms and respond surface methodology [14–18]. Researchers utilized diverse modeling techniques to predict the thermal conductivity of nanofluids, as summarized in tab. 1. ANN modeling has gained popularity among these methods to investigate nanofluid behavior and forecast thermophysical properties. For instance, Long Li *et al*.[19] Conducted experiments to investigate the viscosity and thermal conductivity of Al_2O_3/EG nanofluids with different mass fractions (0% and 2%) and T ranging from 20°C to 90°C. An ANN model was developed by them that achieved high coefficients of determination (R^2) of 0.9984 for viscosity and 0.9997 for thermal conductivity. Similarly, Alireza Akhgar *et al*.[20] Used an ANN model to analyse the thermal conductivity of MWCNT-TiO_2/water-EG nanofluids, demonstrating that the ANN approach outperformed traditional correlations in predicting experimental results.

The test dataset produced a mean squared error (MSE) of 0.019753449 and a mean absolute error (MAE) of 0.0117. Further, Ashutosh Pare *et al*. [21] Investigated the thermal conductivity of nanofluids consisting of distilled water with Al_2O_3, Chou, and Zinc oxide (ZnO). They varied the nanoparticle Φ between 0.02% and 2% and the T range between 20°C and 90°C. Compared to their proposed ANN model and theoretical correlations, their experimental results demonstrated accuracy levels within 2%. Nguyen *et al*. [22] Examined the thermal conductivity of Graphene Oxide (GO) and Silicon dioxide (SiO_2) / water hybrid nanofluids. Based on experimental data, they created a numerical correlation and an ANN model. The ANN model achieved an R^2 of 0.999, while the numerical model had an R^2 of 0.9. Their proposed correlation was based on a relationship between biases and preferences, which showed promising results. Rostami *et al*.[23] An MWCNT-Chou/water nanofluid was synthesized, and an ANN model was used to predict its thermal conductivity. They observed a significant enhancement of approximately 30% in thermal conductivity under specific conditions with a Φ of 0.6% and T of 50°C. Arani *et al*. [24] Employed an ANN to predict the response variable (R^2 = 0.997) for Magnesium Oxide (MgO) /water nanofluid heat transfer, considering MgO particle size and Reynolds number. Yu-Ming Chu *et al*.[25] Conducted experiments and employed response surface methods (RSM) and ANN models to investigate the rheological behavior of hybrid nanofluids with

MWCNT-TiO_2/5W40. The ANN model demonstrated a maximum error below 5% with an R^2 value of 0.999. Shaopeng Tian et al.[26] Predicted the thermal conductivity of GO-Al_2O_3/water-EG hybrid nanofluids using a perceptron feed-forward ANN. The trainbr algorithm showed that the ANN model had been well-trained and had a correlation coefficient of 0.999 for thermal conductivity.

Table 1. Summary of researches conducted for prediction of nanofluid properties.

Author	Nanofluid	Purpose	Method
R. Dinesh *et al*.[27]	GO-MO nano lubricants	Thermal and rheological behaviour of nanofluid	ANN
Mehdi Jamei *et al*.[28]	Oil based nanofluids	Thermal conductivity prediction	ANN/ RSM
Tareq Salameh *et al*. [29]	Al_2O_3/SiO_2 nanofluid	Thermophysical properties of nanofluid	Fuzzy logic model and
Yu Jiang *et al*.[30]	Al_2O_3/deionized water	Thermal conductivity prediction of nanofluids	Fuzzy lookup table method
Surendra D *et al*.[31]	Ag/ZnO hybrid nanofluids	Prediction of thermal conductivity of nanofluids	ANN
Chuan Sun *et al*.[32]	WO_3/Liquid Paraffin	Thermal conductivity prediction	Fuzzy Logic /ANN
Ammar H *et al*.[33]	Al_2O_3, CuO and TiO_2)/ Water	Prediction the thermal conductivity of nanofluids	ANN

As per existing literature, a significant portion of researchers has dedicated their efforts to examining and forecasting the thermophysical characteristics of nanofluids utilizing water and EG. Nevertheless, there has been relatively scant exploration into assessing the thermal conductivity of nanofluids incorporating oil as the base fluid. This study endeavors to analyze the improvement in thermal conductivity within SAE10W oil nanofluids through the incorporation of graphene nanoplatelets (GnPs). Furthermore, the aim is to establish a highly precise predictive model utilizing ANN and RSM techniques based on experimental data.

2. Materials and Methods

2.1. Preparation of nanofluid

The functionalized GnPs were procured from Cheap Tubes Inc., located in Grafton, VT, USA, in the form of nanosheets. These GnPs exhibit a specific surface area of 700 m²/g, a thickness of 4 nm and lateral dimensions of 2 µm. They belong to grade 4O+ and possess a purity of 99%. Graphene was chosen due to its lower density and superior thermal conductivity properties when compared to metallic materials. The automotive damper oil with a grade SAE 10W was selected as a base fluid. The preparation of GnPs/SAE10W oil nanofluids involved a two-step method. The GnPs are initially suspended in SAE10W oil with concentrations of 0.050%, 0.075%, 0.100%, 0.150%, and 0.150%. Generally, the higher the Φ, the more pronounced the sedimentation and agglomeration of nanoparticles in the fluids [34–36]. Therefore, lower ranges [0.050% to 0.150%] of Φ were selected for this study to address this issue.

2.2. Thermal conductivity measurement

The thermal conductivity of the GnPs/SAE10W oil nanofluid was assessed employing a Hot Disk Thermal Constants Analyzer (Hot Disk-Instrument TPS 2500S). This analyser has the capability to measure thermal conductivity within the range of 0.005 to 1800 W/mK with an accuracy exceeding 5%. In order to calibrate the instrument, deionized water was used in a temperature range of 20°C to 80°C before measurements of nanofluid thermal conductivity were performed. The objective of this calibration was to evaluate the accuracy and precision of the instrument's sensor. The refprop 9.0

database [37] was compared with the acquired data, and the measurements indicated an accuracy of less than 1% that complied with the manufacturer's declared accuracy standards.

3. ANN modelling

The use of ANNs as a method for addressing nonlinear systems has become widely accepted in recent years due to their significant advances in the field. The popularity of these approaches is attributed to their exceptional accuracy, cost-effectiveness and efficiency in terms of time. The parallel processing abilities of neural networks, which are comparable to those of the human brain enable a more profound comprehension of intricate relationships between input and output variables. A feed-forward perceptron (ANN) with the Levenberg-Marquardt (Trainlm) algorithm was used to predict the thermal conductivity of GnPs/SAE10W oil nanofluids.

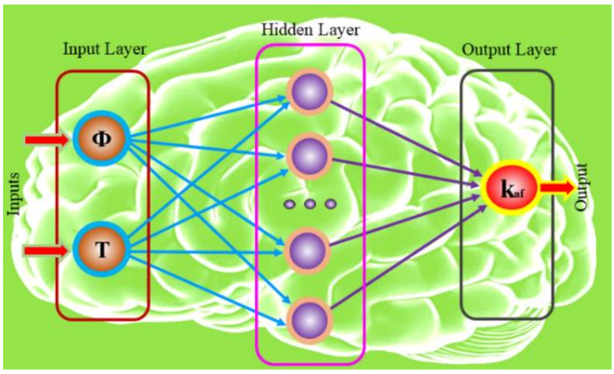

Fig. 1. ANN architecture

As illustrated in fig. 1, the architecture of the artificial neural network (ANN) comprises three layers: the input layer, hidden layer and output layer to minimize prediction errors. The use of feed-forward ANNs for function estimation is particularly advantageous due to their significant promise in this area[38, 39]. The ANN model was implemented using MATLAB software, which is a reliable platform for creating and training the neural network model. The next step involved determining the optimal number of neurons in each layer. The input and output data can determine the number of neurons in a layer. This study considered two inputs: Φ, T and the output was thermal conductivity. The objective is to predict the thermal conductivity of the GnPs/SAE10W nanofluids. For training and testing, the dataset contains 35 data points that were obtained from 5 values of Φ and 7 values of T. tab. 2 shows an experimental dataset that was used to train the ANN. The dataset is divided into three segments, and 70% of it is dedicated to training, 15% to validation, and 15% to testing[40]. In this study, the correlation between the characteristic parameters of the ANN neuron, including weight (w_j), bias (b_j), activation function (f), the input signal (x_i) and output signal (y) is achieved through the following Eq. (1) [41]. The activation function used is the tangent sigmoid as described in Eq. (2) [41]. Moreover, the purelin activation function is utilized for the output layer.

$$y_j = f\left(\sum_{i=1}^{n} w_{j,i}x_i + b_j\right) \tag{1}$$

$$f(x) = \frac{1}{1+exp(-x)} \tag{2}$$

The most effective number of neurons in the hidden layer was determined through iterative testing involving various neuron numbers and evaluating their performance. The performance measures for each neuron number are determined through training, validation, testing and overall performance. The minimum MSE and maximum R^2 are the two metrics used to evaluate the performance of the ANN modeling approach. By minimizing the MSE value to zero and approaching an R^2 value of 1, a model's accuracy can be improved. The R^2 and MSE are expressed [19] by Eqs. (3) and (4).

$$R^2 = 1 - \frac{\sum_{i=1}^{N}\left((k_{nf})_{(Experimental\,data)} - (k_{nf})_{(predicted\,data)}\right)^2}{\sum_{i=1}^{N}\left((k_{nf})_{(Experimental\,data)}\right)^2} \quad (3)$$

$$MSE = \frac{1}{N}\sum_{i=1}^{N}\left((k_{nf})_{(Experimental\,data)} - (k_{nf})_{(predicted\,data)}\right)^2 \quad (4)$$

Table 2. Thermal conductivity of GnPs/SAE10W oil nanofluids (w/mK)

Φ (%) / T(°C)	0	0.05	0.075	0.1	0.125	0.15
20	0.1382	0.1641	0.1662	0.1692	0.1698	0.1711
30	0.1362	0.1656	0.1667	0.1699	0.1701	0.1723
40	0.1348	0.1663	0.1681	0.1704	0.1711	0.1732
50	0.1336	0.1669	0.1697	0.1711	0.1723	0.1741
60	0.1323	0.1680	0.1715	0.1724	0.1739	0.1753
70	0.1304	0.1701	0.1732	0.1748	0.1761	0.1771
80	0.1274	0.1728	0.1745	0.1759	0.1781	0.1796

4. Result and Discussion

4.1. Experimental analysis

fig. 2 (a), illustrates the relationship between Φ, T and thermal conductivity for GnPs/SAE10W oil nanofluids. Experimental data points that represent these relationships are also included. The horizontal axis (X) represents the Φ of the GnPs, while the vertical axis (Y) indicates the thermal conductivity of the nanofluids. With rising T, the base fluid's thermal conductivity decreases from 0.1382 W/mK to 0.1274 W/mK, which is due to the fluid's inherent properties. Experimental results demonstrate improved thermal conductivity of SAE10W oil with increasing Φ of GnPs and T. The thermal conductivity of GnPs/SAE10W oil nanofluids shows a significant enhancement from 0.1641 W/mK to 0.1728 W/mK at a Φ of 0.050%. This phenomenon can be observed in the T range of 20°C to 80°C. Subsequently, within the same T range, the thermal conductivity of nanofluid undergoes the following changes: from 0.1662 W/mK to 0.1728 W/mK at Φ of 0.075%, from 0.1692 W/mK to 0.1759 W/mK at Φ of 0.100%, from 0.1698 W/mK to 0.1781 W/mK at Φ of 0.125%, and from 0.1711 W/mK to 0.1796 W/mK at Φ of 0.150%.

(a) (b)

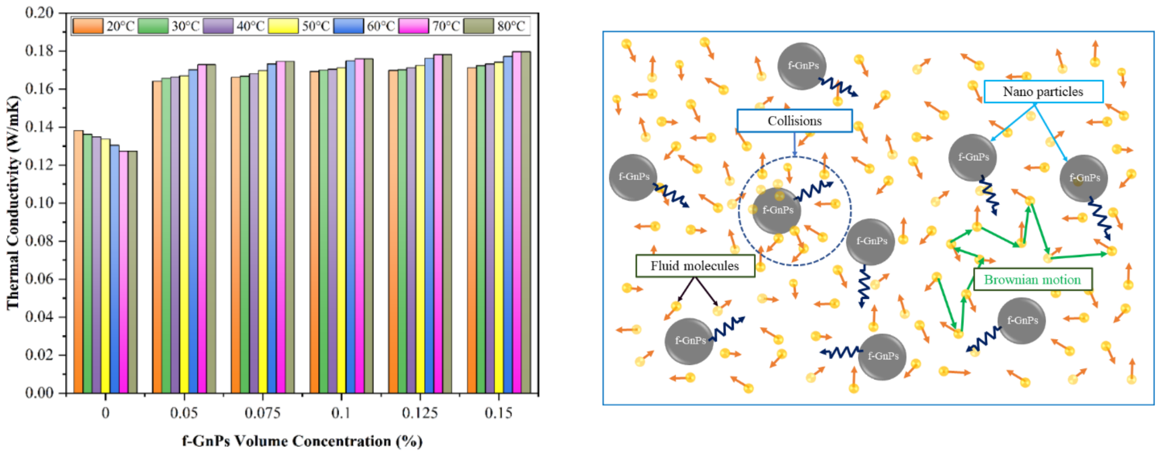

Fig. 2. (a) Effects of Φ and T on k of the GnPs/SAE10W oil nanofluids, (b) Mechanism for thermal conductivity enhancement in nanofluids [42].

The findings show that thermal conductivity is improving as the Φ of GnPs/SAE10W oil nanofluids increases within the specified T range. Notably, the nanofluids exhibit thermal conductivity enhancements ranging from approximately 19% to 41% within the selected T range and Φ. As shown in fig. 2(b), the mechanisms responsible for enhancing the thermal conductivity of the GnPs/SAE10W oil nanofluid are the ones responsible for the T-dependent effects on nanofluids.

The mobility of GnPs is significantly increased as the T rises, and as the intermolecular bonds within the fluid layers weaken. The heightened mobility of nanoparticles results in more frequent collisions between their surface atoms and fluid molecules[43, 44]. Consequently, there is a substantial improvement in overall heat conduction[45, 46]. The rise in T causes more Brownian motion, which is the random movement of fluid molecules and GnPs. This makes the GnPs/SAE10W oil nanofluids better at conducting heat. Furthermore, the presence Φ of GnPs improves the thermal conductivity of GnPs/SAE10W oil nanofluids. This is due to nanoparticles' higher thermal conductivity compared to the base fluid. As the Φ of GnPs increases, more nanoparticles are present in the nanofluid, leading to a more significant enhancement in thermal conductivity. This phenomenon has a significant impact on the thermal conductivity increase in f-GnPs/SAE10W oil nanofluids.

4.2. ANN model performance analysis

The performance outcomes for the ANN model, considering various neuron numbers for predicting nanofluid thermal conductivity, are presented in tab. 3. The correlation coefficients for different neuron numbers such as MSE and R^2 values are displayed in this table. In the first column, the neuron numbers are represented with each row representing the correlation coefficient of a specific neuron number. These coefficients are a reflection of the correlations that were observed in the train, test, validation and overall datasets. The ANN model's performance is evaluated for up to 20 neurons. The results in tab. 3 show that the best ANN model for forecasting the thermal conductivity of f-GnPs/SAE10W oil nanofluids has a single hidden layer with 12 neurons. The selection of this effective model is based on attaining the lowest MSE and highest R^2 values. This configuration consistently demonstrated superior performance across all metrics (MSE and R^2) for training, testing, validation, and overall dataset evaluation. In fig. 3, an ANN model with optimized structures is used to predict the thermal conductivity of GnPs/SAE10W oil.

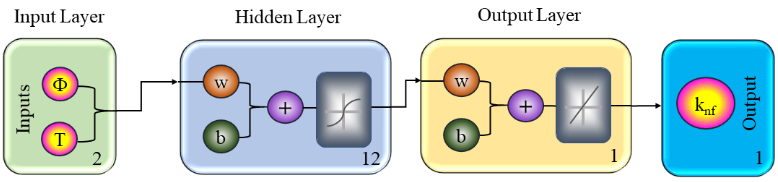

Fig. 3. The optimal model of ANN architecture for prediction of thermal conductivity

fig. 4 (a), depicts the performance graph, illustrating the fluctuation of Mean Squared Error (MSE) throughout the training stages for predicting the thermal conductivity of the f-GnP/SAE10W oil nanofluid. The horizontal axis represents epochs (X), while the vertical axis indicates the MSE during the training of the ANN model. With an increasing number of epochs, the observed trend consistently reveals a decrease in MSE values, ultimately reaching a point of stability. This trend indicates effective training of the neural network. Moreover, MSE's steady behavior even after more epochs confirms that the model is not overfitting. The best validation performance is represented by a small green circle in fig. 4 (a), which is achieved for the thermal conductivity of nanofluid with the lowest MSE for the validation dataset at epoch 7, measuring 2.5381e-07. The histograms of the error between the experimental data and predicted ANN data for the thermal conductivity of the GnPs/SAE10W oil nanofluids after training a feed-forward neural network are also shown in fig. 4(b).

Neuron number	MSE			R^2			
	Train	Validation	Test	Train	Validation	Test	Overall
6	8.05E-08	2.73E-07	1.09E-06	0.99567	0.99602	0.98227	0.9912
7	4.03E-08	4.88E-08	6.73E-07	0.99861	0.99887	0.98718	0.99528
8	5.11E-07	5.06E-08	4.91E-07	0.9825	0.98555	0.99259	0.98359
9	1.07E-07	2.66E-07	3.17E-07	0.99513	0.9888	0.99583	0.99418
10	9.25E-13	4.23E-07	8.97426-7	1	0.99379	0.96972	0.99331
11	1.44E-10	1.25E-06	7.58E-07	0.99999	0.97938	0.95829	0.99003
12	**2.27E-08**	**2.53E-07**	**9.33E-07**	**0.99946**	**0.9965**	**0.99753**	**0.99761**
13	3.29E-08	5.04E-07	6.79E-07	0.99883	0.99509	0.98002	0.9936
14	1.53E-08	2.92E-07	5.30E-07	0.99954	0.98288	0.98525	0.9954
15	1.49E-08	6.37E-07	2.69E-07	0.99937	0.99538	0.9886	0.9949
16	2.90E-11	6.51E-07	1.12E-06	1	0.98852	0.96014	0.99207
17	2.96E-08	1.09E-06	6.80E-07	0.99909	0.98801	0.97947	0.99185
18	2.44E-13	8.34E-07	8.24E-07	1	0.98795	0.98483	0.99174
19	1.30E-11	6.56E-07	2.97E-07	1	0.9715	0.99742	0.99571
20	2.76E-08	2.32E-07	7.16E-07	0.99914	0.97504	0.82964	0.99422

Table 3. The neural network performance results in different neuron numbers

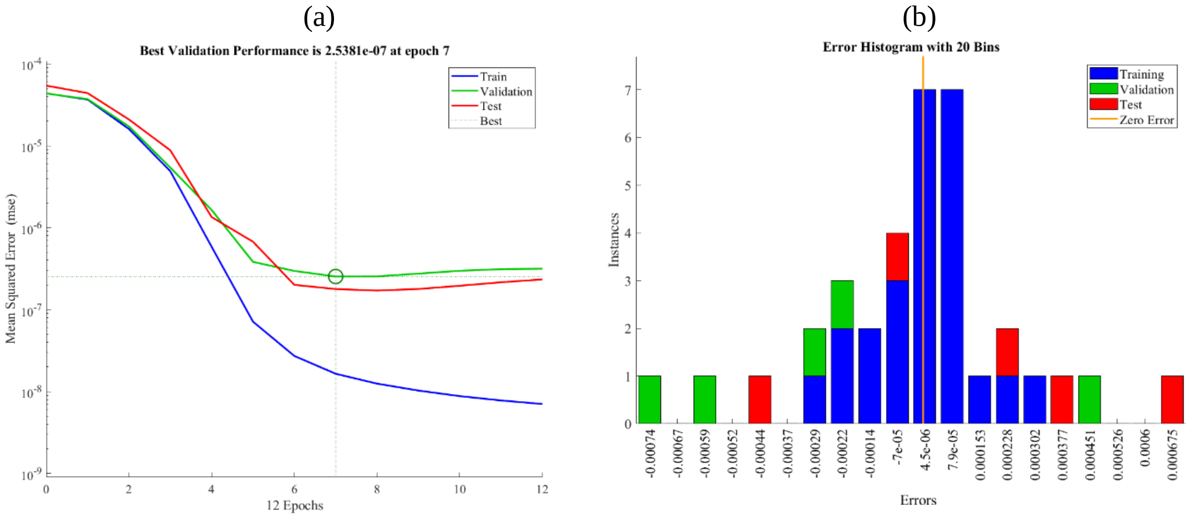

Fig. 4. (a) ANN model - MSE plot, (b) ANN error histogram

The histogram graph has a horizontal axis for errors (X) and a vertical axis for instances (Y). The histograms display the distribution of errors using bar charts that illustrate various error values. An increased occurrence of data errors near the zero error line suggests a reduced error rate within the system, which indicates the successful training of the ANN model. The elevated bars next to the zero-error line serve as evidence of the method's ability to closely align the model output with the experimental data. A zero line indicates an error rate of less than 1% in most cases. This observation confirms the accuracy and reliability of the chosen approach in predicting thermal conductivity for GnPs/SAE10W oil nanofluids.

As shown in fig. 5(a), the horizontal axis represents experimental data (X), and the vertical axis represents predicted ANN data (Y). It might refer to the relationship between experimental data on the thermal conductivity of GnPs/SAE10W oil nanofluids and predicted ANN data. The results presented encompass the performance of the models in training, validation, testing, and the overall dataset, showing exceptional fits close to the equator line. Furthermore, R^2 is offered for every dataset. The closeness of the R^2 to one indicates a strong relationship between the experimental and predicted data sets. It is notable that the regression coefficients for all the datasets used in the model are above 0.99, which further confirms the strong correlation between the experimental and predicted data sets.

(a) (b)

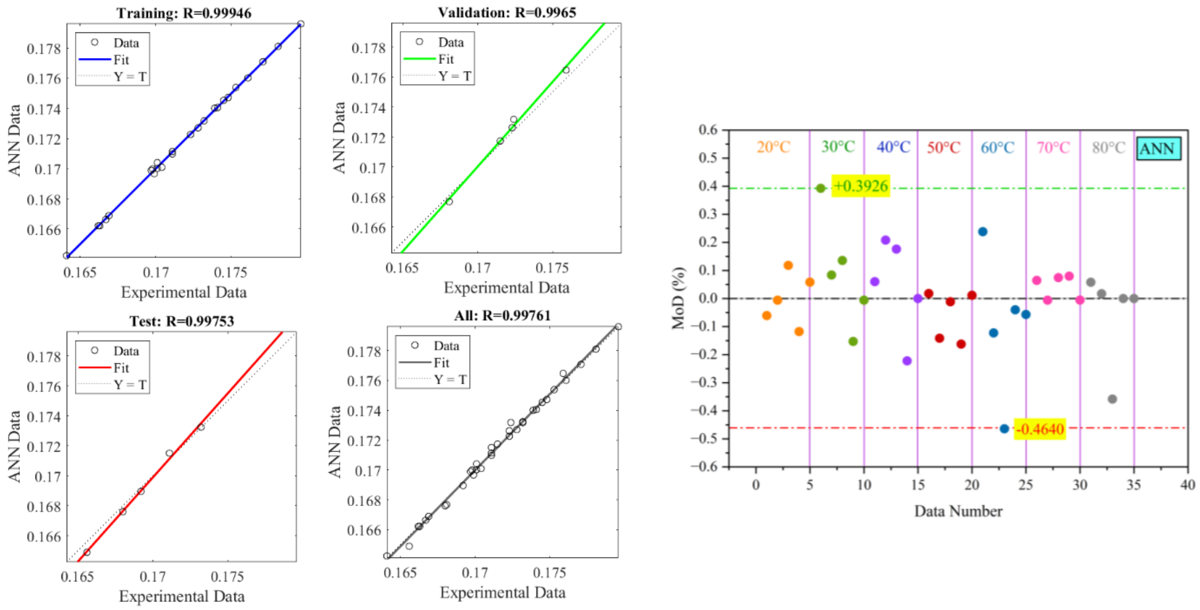

Fig. 5.(a) The correlation coefficient and regression diagram, (b) MOD for ANN

The Margin of Deviation (MoD) can be used to assess the accuracy of the proposed ANN model, which quantifies the difference between experimental data and ANN predictions. In fig. 5(b), the formula provided [20] in Eq. (5) is employed to compute the MoD for the ANN data in predicting the experimental data. The MoD analysis results indicate a high level of accuracy for the network, with only a few instances falling within the positive and negative ranges, ranging from +0.3926% to -0.4640%.

$$\text{Margin of deviation}(\%) = \left[\frac{\left((k_{nf})_{(\text{Experimental})} - (k_{nf})_{(\text{Predicted})}\right)}{(k_{nf})_{(\text{Experimental})}}\right] X\ 100 \qquad (5)$$

4.3. RSM model performance analysis

Experimental data was used to develop a mathematical model that predicts the behavior of the nanofluid using RSM techniques. The input variables used in this technique are the Φ of nanomaterials and T, with the thermal conductivity of nanofluid representing the third dimension on the surface. The 3D-fitted surface for the experimentally measured data is shown in fig. 6(a). The black dots on its representation closely match the 3D- fitted surface and accurately depict the behavior of GnPs/SAE10W oil nanofluid. A third-order function for both input variables was selected after experimenting with different orders of functions. The resulting equation for the fitted surface is presented in Eq. (6).

$$k_{nf}(\Phi, T)=0.1712+0.0024\,\Phi+0.0025T-0.0003\Phi^2+0.00069T^2+0.0001T^3 \quad (6)$$

Eq. (6) is pertinent for the range of 20°C ≤ T ≤ 80°C, 0.050 ≤ Φ ≤ 0.150%. This correlation predicts the thermal conductivity of GnPs/SAE10W oil nanofluids. The plot shows that the thermal conductivity of nanofluid is directly related to Φ and T. These findings emphasize the significance of Φ and T in determining the thermal conductivity of GnPs/SAE10W oil nanofluids.

(a) (b)

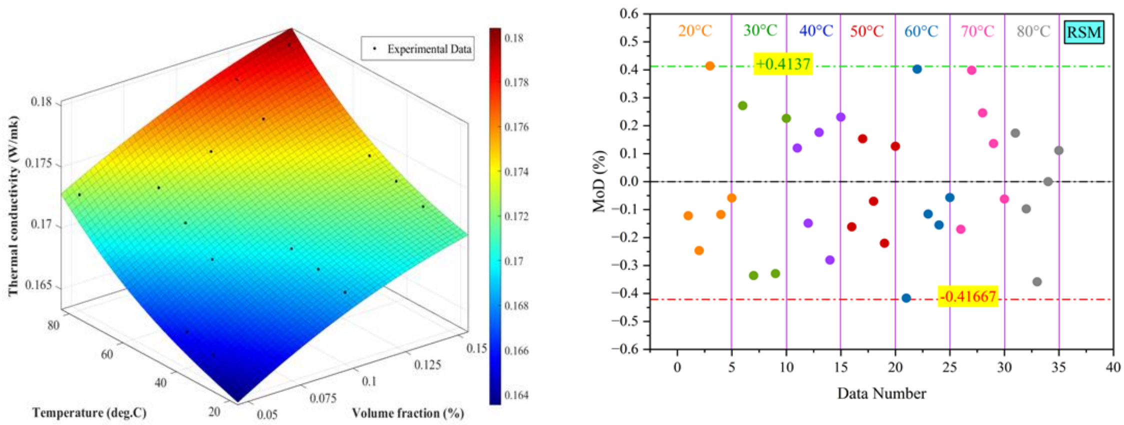

Fig. 6. (a) 3D surface fitted graph, (b) MOD for RSM

The correlation coefficients for thermal conductivity of nanofluid were 3D surface-fitted and resulted in an R2 value of 0.9877 with an RMSE of 0.0005. The correlations are well-fitted and highly accurate, as demonstrated by the high R2 and lowest RMSE values. Fig. 6(b) shows the distribution of MoD for the RSM technique, with a range of MoD values between 0.4137% and -0.4166%.

In the results of the ANN and RSM techniques, the MSE is 2.5381e-07 and 0.0005, while the MODs are 0.3926% and 0.4137%, respectively. The ANN and RSM techniques also exhibit correlation coefficients of 0.99761 and 0.9877, respectively. Fig. 7(a) shows that the RSM and ANN techniques produce results that are similar to experimental ones. The absolute error of the ANN method is smaller than that of the RSM method in most data points, as shown in fig. 7(b).

(a) (b)

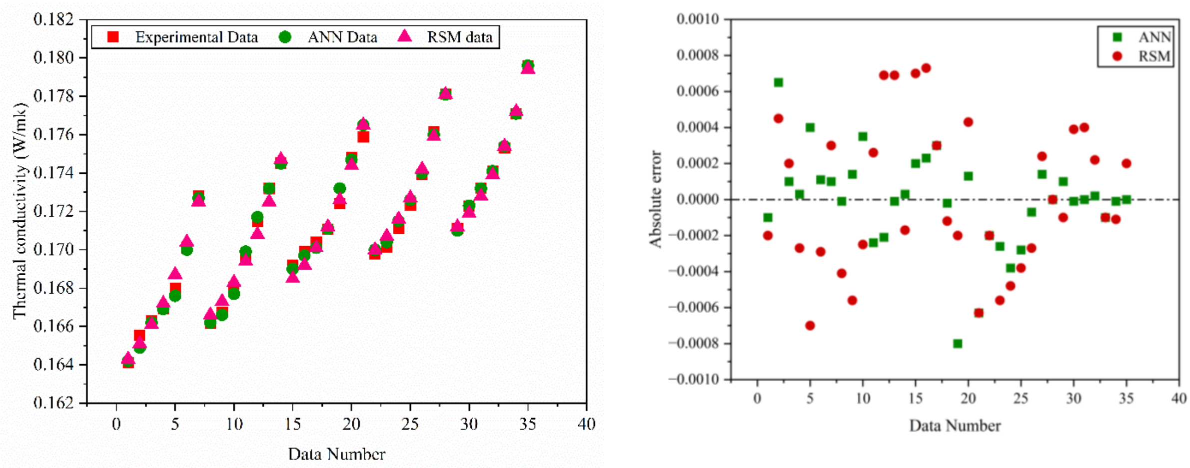

Fig. 7. (a) Comparison of the Experimental, ANN, and RSM data, (b) Absolute errors in ANN and RSM data

4. Conclusion

The thermal conductivity of GnPs/SAE10W oil nanofluid was measured at various volume concentrations and temperatures. The results show that the thermal conductivity of GnPs/SAE10W oil nanofluids has improved from 19% to 41%. This improvement in thermal conductivity is attributed to the enhanced heat transfer properties of the nanofluids. Furthermore, a novel and generalized approach to ANN and a mathematical model have been developed for predicting the thermal conductivity of the nanofluid. In the ANN model, the best performance was reported using a trainlm algorithm with 12 neurons in the hidden layer, as R^2 and MOD were 0.99761 and 0.3926%, respectively. The mathematical model developed by RSM techniques with R^2 and MOD was 0.9877 and 0.4137%, respectively. The ANN model showed higher accuracy in predicting the thermal conductivity of the GnPs/SAE10W oil nanofluid compared to the mathematical model.

Future perspective

The proposed research work has identified an approach for modeling the thermal conductivity properties of nano damper oils. The model has been formulated for GnPs based nanofluids. The modeling algorithm and utilization of ANN/RSM techniques can be deployed for similar heat transfer applications, such as automotive radiators, solar panels, etc.

Nomenclature

k - thermal conductivity [$Wm^{-1}K^{-1}$]
T - temperature [°C]
R^2 - coefficient of determination [-]
n - number of neurons [-]
N - number of sample data [-]

Greek symbols
Φ - volume fraction [%]

Subscripts
nf - nanofluid

References

[1] Shah, Z., et al., Heat Transfer Intensification of Nanomaterial with Involve of Swirl Flow Device Concerning Entropy Generation, *Sci. Rep.*, *11* (2021), 1, pp. 1-15, doi: 10.1038/s41598-021-91806-y.

[2] Gonçalves, I., et al., Thermal Conductivity of Nanofluids: A Review on Prediction Models, Controversies And Challenges, *Appl. Sci.*, *11* (2021), 6, pp.1-26, doi: 10.3390/app11062525.

[3] Kondakrindi, K.R., et al., Experimental Investigation on The Influence of Nanofluids Used As Heat Transfer Fluid in Phase Change Material Based Thermal Energy Storage System, *Therm. Sci.*, *25* (2021), pp. 643-652, doi: 10.2298/TSCI191004060R.

[4] Huang, H., et al., Study of A Novel Ternary Second-Order Viscosity Model on Al_2O_3-Water Nanofluid, *Therm. Sci.*, *27* (2023), 5, pp. 4223-4234, doi: 10.2298/TSCI220926064H.

[5] Hamze, S., et al., Few-Layer Graphene-Based Nanofluids with Enhanced Thermal Conductivity, *Nanomaterials*, *10* (2020), 7, pp. 1-21, doi: 10.3390/nano10071258.

[6] Hemmat Esfe, M., et al., Thermal Conductivity of MWCNT-TiO_2/Water-EG Hybrid Nanofluids: Calculating The Price Performance Factor (PPF) Using Statistical And Experimental Methods (RSM), *Case Stud. Therm. Eng.*, *48* (2023), April, pp. 103094, doi: 10.1016/j.csite.2023.103094.

[7] Khan, Y., et al., Classification, Synthetic, and Characterization Approaches to Nanoparticles, and Their Applications in Various Fields of Nanotechnology: A Review, *Catalysts*, *12* (2022), 11, doi: 10.3390/catal12111386.

[8] Qiu, L., et al., A Review of Recent Advances in Thermophysical Properties at The Nanoscale: From Solid State to Colloids, *Phys. Rep.*, *843* (2020), pp. 1-81, doi: 10.1016/j.physrep.2019.12.001.

[9] Hemmat Esfe, M., et al., Rheological Behavior of 10W40 Base Oil Containing Different Combinations of MWCNT-Al_2O_3 Nanoparticles and Determination of The Target Nano-Lubricant For Industrial Applications, *Micro Nano Syst. Lett.*, *11* (2023), 1, doi: 10.1186/s40486-023-00179-6.
[10] JASIM, Q.K., et al., Improving Thermal Performance Using Al_2O_3-Water Nanofluid in a Double Pipe Heat Exchanger Filling with Porous Medium, *Therm. Sci.*, *24* (2020), 6, pp. 4267-4275, doi: 10.2298/TSCI190602056J.
[11] Nfawa, S.R., et al., Novel use of MgO Nanoparticle Additive For Enhancing The Thermal Conductivity of CuO/Water Nanofluid, *Case Stud. Therm. Eng.*, *27* (2021), June, pp. 101279, doi: 10.1016/j.csite.2021.101279.
[12] Yıldız, G., et al., A Review of Stability, Thermophysical Properties and Impact of Using Nanofluids on The Performance of Refrigeration Systems, *Int. J. Refrig.*, *129* (2021), pp. 342-364, doi: 10.1016/j.ijrefrig.2021.05.016.
[13] Barai, D.P., et al., Artificial Neural Network For Prediction of Thermal Conductivity of RGO–Metal Oxide Nanocomposite-Based Nanofluids, *Neural Comput. Appl.*, *34* (2022), 1, pp. 271-282, doi: 10.1007/s00521-021-06366-z.
[14] Nawaz, A., Kumar, P., Optimization of Process Parameters of Lagerstroemia Speciosa Seed Hull Pyrolysis Using a Combined Approach of Response Surface Methodology (RSM) and Artificial Neural Network (ANN) For Renewable Fuel Production, *Bioresour. Technol. Reports*, *18* (2022), pp. 101110, doi: https://doi.org/10.1016/j.biteb.2022.101110.
[15] Nawaz, A., Kumar, P., Thermal Degradation of Hazardous 3-Layered COVID-19 Face Mask Through Pyrolysis: Kinetic, Thermodynamic, Prediction Modelling Using ANN and Volatile Product Characterization, *J. Taiwan Inst. Chem. Eng.*, *139* (2022), September, pp. 104538, doi: 10.1016/j.jtice.2022.104538.
[16] Alhadri, M., et al., Response Surface Methodology (RSM) and Artificial Neural Network (ANN) Simulations For Thermal Flow Hybrid Nanofluid Flow with Darcy-Forchheimer Effects, *J. Indian Chem. Soc.*, *99* (2022), 8, pp. 100607, doi: https://doi.org/10.1016/j.jics.2022.100607.
[17] Alfaleh, A., et al., Predicting Thermal Conductivity and Dynamic Viscosity of Nanofluid By Employment of Support Vector Machines: A Review, *Energy Reports*, *10* (2023), pp. 1259-1267, doi: 10.1016/j.egyr.2023.08.001.
[18] Azimi, M., Vakilipour, S., The 2-D Cu-Water Nanofluid-Flow and Heat Transfer Over an Inclined Wall And Between Two Inclined Walls- The Numerical Solution of PDE And ODE, *Therm. Sci.*, *26* (2022), 6, pp. 5053-5067, doi: 10.2298/TSCI220129051A.
[19] Li, L., et al., Stability, Thermal Performance and Artificial Neural Network Modeling of Viscosity and Thermal ConductivityoOf Al_2O_3-Ethylene Glycol Nanofluids, *Powder Technol.*, *363* (2020), pp. 360-368, doi: 10.1016/j.powtec.2020.01.006.
[20] Akhgar, A., et al., Developing Dissimilar Artificial Neural Networks (ANNs) To Prediction The Thermal Conductivity of MWCNT-TiO_2/Water-Ethylene Glycol Hybrid Nanofluid, *Powder Technol.*, *355* (2019), pp. 602-610, , doi: 10.1016/j.powtec.2019.07.086.
[21] Pare, A., Ghosh, S.K., A Unique Thermal Conductivity Model (ANN) For Nanofluid Based on Experimental Study, *Powder Technol.*, *377* (2021), pp. 429-438, doi: 10.1016/j.powtec.2020.09.011.
[22] Nguyen, Q., et al., A Novel Correlation To Calculate Thermal Conductivity of Aqueous Hybrid Graphene Oxide/Silicon Dioxide Nanofluid: Synthesis, Characterizations, Preparation, and Artificial Neural Network Modeling, *Arab. J. Sci. Eng.*, *45* (2020), 11, pp. 9747-9758, doi: 10.1007/s13369-020-04885-w.
[23] Rostami, S., et al., Measurement of The Thermal Conductivity of MWCNT-CuO/Water Hybrid Nanofluid Using Artificial Neural Networks (ANNs), *J. Therm. Anal. Calorim.*, *143* (2021), 2, pp. 1097-1105, doi: 10.1007/s10973-020-09458-5.
[24] Arani, A.A.A., et al., Statistical Analysis of Enriched Water Heat Transfer with Various Sizes of MgO Nanoparticles Using Artificial Neural Networks Modeling, *Phys. A Stat. Mech. its Appl.*, *554* (2020), pp. 123950, doi: 10.1016/j.physa.2019.123950.
[25] Chu, Y.-M., et al., Examining Rheological Behavior of MWCNT-TiO_2/5W40 Hybrid Nanofluid Based on Experiments and RSM/ANN Modeling, *J. Mol. Liq.*, *333* (2021), pp.

115969, doi: https://doi.org/10.1016/j.molliq.2021.115969.
[26] Tian, S., et al., Using Perceptron Feed-Forward Artificial Neural Network (ANN) For Predicting The Thermal Conductivity of Graphene Oxide-Al_2O_3/Water-Ethylene Glycol Hybrid Nanofluid, *Case Stud. Therm. Eng.*, *26* (2021), May, doi: 10.1016/j.csite.2021.101055.
[27] Dinesh, R., et al., An Experimental Investigation and Comprehensive Modelling of Thermal and Rheological Behaviour of Graphene Oxide Nano Platelets Suspended Mineral Oil Nano Lubricant, *J. Mol. Liq.*, *347* (2022), pp. 118357, doi: 10.1016/j.molliq.2021.118357.
[28] Jamei, M., et al., On The Thermal Conductivity Assessment of Oil-Based Hybrid Nanofluids Using Extended Kalman Filter Integrated with Feed-Forward Neural Network, *Int. J. Heat Mass Transf.*, *172* (2021), pp. 121159, doi: 10.1016/j.ijheatmasstransfer.2021.121159.
[29] Salameh, T., et al., Fuzzy Modeling And Particle Swarm Optimization of Al_2O_3/SiO_2 Nanofluid, *Int. J. Thermofluids*, *10* (2021), doi: 10.1016/j.ijft.2021.100084.
[30] Jiang, Y., et al., Propose A New Approach of Fuzzy Lookup Table Method to Predict Al_2O_3/Deionized Water Nanofluid Thermal Conductivity Based on Achieved Empirical Data, *Phys. A Stat. Mech. its Appl.*, *527* (2019), pp. 121177, doi: 10.1016/j.physa.2019.121177.
[31] Barewar, S.D., et al., Experimental Investigation of Thermal Conductivity and Its ANN Modeling For Glycol-Based Ag/ZnO Hybrid Nanofluids with Low Concentration, *J. Therm. Anal. Calorim.*, *139* (2020), 3, pp. 1779-1790, doi: 10.1007/s10973-019-08618-6.
[32] Sun, C., et al., Liquid Paraffin Thermal Conductivity with Additives Tungsten Trioxide Nanoparticles: Synthesis and Propose A New Composed Approach of Fuzzy Logic/Artificial Neural Network, *Arab. J. Sci. Eng.*, *46* (2021), 3, pp. 2543-2552, doi: 10.1007/s13369-020-05151-9.
[33] Elsheikh, A.H., et al., An Artificial Neural Network Based Approach For Prediction The Thermal Conductivity of Nanofluids, *SN Appl. Sci.*, *2* (2020), 2, pp. 1-11, doi: 10.1007/s42452-019-1610-1.
[34] Souza, R.R., et al., Recent Advances on The Thermal Properties and Applications of Nanofluids: From Nanomedicine to Renewable Energies, *Appl. Therm. Eng.*, *201* (2022), November 2021,doi: 10.1016/j.applthermaleng.2021.117725.
[35] Yılmaz Aydın, D., Gürü, M., Nanofluids: preparation, stability, properties, and thermal performance in terms of thermo-hydraulic, thermodynamics and thermo-economic analysis, *Journal of Thermal Analysis and Calorimetry*, vol. 147 (2022),14. pp. 7631–7664, doi: 10.1007/s10973-021-11092-8.
[36] Le Ba, T., et al., Review on the recent progress in the preparation and stability of graphene-based nanofluids, *Journal of Thermal Analysis and Calorimetry*, vol. 142 (2020), no. 3, pp. 1145–1172, doi: 10.1007/s10973-020-09365-9.
[37] Lemmon, E.W., et al., NIST Standard Reference Database 23: Reference Fluid Thermodynamic And Transport Properties-REFPROP, Version 9.1, Standard Reference Data Program, *Natl. Inst. Stand. Technol. Gaithersburg, MD*, (2013), pp. 1-3.
[38] Ibrahim, M., et al., Study of Capabilities of The ANN And RSM Models to Predict The Thermal Conductivity of Nanofluids Containing SiO_2 Nanoparticles, *J. Therm. Anal. Calorim.*, *145* (2021), 4, pp. 1993-2003, doi: 10.1007/s10973-021-10674-w.
[39] Hema, M., et al., Prediction of Viscosity of MWCNT-Al_2O_3 (20:80)/SAE40 Nano-Lubricant Using Multi-Layer Artificial Neural Network (MLP-ANN) Modeling, *Eng. Appl. Artif. Intell.*, *121* (2023), January, pp. 105948, doi: 10.1016/j.engappai.2023.105948.
[40] Esfe, M.H., et al., Optimization and Design of ANN with Levenberg-Marquardt Algorithm to Increase The Accuracy in Predicting the Viscosity of SAE40 Oil-Based Hybrid Nano-Lubricant, *Powder Technol.*, *415* (2023), November 2022, pp. 118097, doi: 10.1016/j.powtec.2022.118097.
[41] Adun, H., et al., A Neural Network-Based Predictive Model For The Thermal Conductivity of Hybrid Nanofluids, *Int. Commun. Heat Mass Transf.*, *119* (2020), October, doi: 10.1016/j.icheatmasstransfer.2020.104930.
[42] Eneren, P., et al., Experiments on Single-Phase Nanofluid Heat Transfer Mechanisms in Microchannel Heat Sinks: A Review, *Energies*, *15* (2022), 7, doi: 10.3390/en15072525.
[43] Iacobazzi, F., et al., An Explanation of The Al_2O_3 Nanofluid Thermal Conductivity Based on The Phonon Theory of Liquid, *Energy*, *116* (2016), pp. 786-794, doi:

10.1016/j.energy.2016.10.027.

[44] Alshikhi, O., Kayfeci, M., Experimental Investigation of Using Graphene Nanoplatelets and Hybrid Nanofluid as Coolant in Photovoltaic Thermal Systems, *Therm. Sci.*, *26* (2022), 1, pp. 195-208, doi: 10.2298/TSCI200524348A.

[45] Milanese, M., et al., An Investigation of Layering Phenomenon at The Liquid–Solid Interface in Cu And CuO Based Nanofluids, *Int. J. Heat Mass Transf.*, *103* (2016), pp. 564-571, doi: 10.1016/j.ijheatmasstransfer.2016.07.082.

[46] Gupta, J., et al., Three-Level Homogeneous Model For The Study of Heat Transfer Mechanism in Metallic Nanofluids, *Phys. B Condens. Matter*, *662* (2023), pp. 414973, doi: https://doi.org/10.1016/j.physb.2023.414973.

RECEIVED DATE: 30.11.2023.
DATE OF CORRECTED PAPER: 16.12.2023.
DATE OF ACCEPTED PAPER: 16.02.2024.